Reversal of radio-frequency-driven spin diffusion by reorientation of the sample spinning axis

Susan M. De Paul,[a] Marco Tomaselli, and Alexander Pines
Materials Sciences Division, Lawrence Berkeley National Laboratory, Berkeley, California 94720 and Department of Chemistry, University of California, Berkeley, California 94720

Matthias Ernst and Beat H. Meier
Laboratory for Physical Chemistry, University of Nijmegen, Toernooiveld, NL-6525 ED Nijmegen, The Netherlands

(Received 14 October 1997; accepted 7 November 1997)

The dipolar Hamiltonian in a rapidly rotating sample is scaled by the second Legendre polynomial of the cosine of the angle between the rotation axis and the static magnetic field. It is, therefore, possible to refocus the spatial polarization-transfer process, often termed spin diffusion, in extended spin systems by reorienting the rotor axis such that the dipolar interaction Hamiltonian changes sign. We present experimental results which demonstrate that a rapid mechanical sample reorientation leads to a time reversal of the ''radio-frequency-driven'' spin diffusion among ^{13}C spins. © *1998 American Institute of Physics.* [S0021-9606(98)03503-X]

The ability to manipulate the nuclear spin Hamiltonian during the course of a nuclear magnetic resonance (NMR) experiment has permitted the observation of a variety of echo effects. The echo experiments by Hahn *et al.*[1] demonstrated that dephasing due to inhomogeneous interactions could be refocused by a single radiofrequency pulse. Spin echoes have also been observed in homogeneously broadened systems. The experiments of Schneider *et al.*[2] and Rhim *et al.*[3] showed that it is possible to induce a ''time reversal'' of the free-induction decay (FID) in a dipolar-coupled spin system, and Llor *et al.*[4] reported the observation of the time reversal of isotropic many-body spin couplings in zero-field NMR.

More recently, several experiments have demonstrated the possibility of refocusing the process of homonuclear polarization transfer, or ''spin diffusion,''[5] in extended spin systems. Exploiting the fact that the truncated dipolar Hamiltonians in the rotating and laboratory frames have opposite signs,[6] Zhang *et al.*[7] designed a pulse sequence to refocus proton spin diffusion in a static sample. Karlsson *et al.*[8] and Tomaselli *et al.*[9] showed that the polarization-transfer process could also be refocused under conditions of magic-angle spinning (MAS)[10,11] by using rotational-resonance recoupling[12,13] or rotor-synchronized multiple-pulse sequences. The formation of such polarization echoes clearly demonstrates the unitary quantum-mechanical nature of the ''spin-diffusion'' process even though it can in some cases be approximated by a diffusion equation.[5, 14–16]

The dependence of the NMR Hamiltonian on both spatial and spin variables[14,17] suggests that the process of spin diffusion should also be reversible by a mechanical sample reorientation. It has previously been shown that a ''magic echo'' of the free-induction decay can be induced in an oriented liquid-crystalline sample by changing the angle between the director and the external magnetic field, $\mathbf{B_0}$.[18] In this communication, we demonstrate that a time reversal of spin diffusion can be achieved by switching the axis of sample rotation during a radio-frequency-driven spin-diffusion experiment.[19]

In rf-driven spin diffusion, a spin-lock field of strength ω_{1S} is applied to the dilute S spins (^{13}C, ^{15}N) during the mixing time.[19,20] This spin-lock field scales the chemical-shift differences among the S spins virtually to zero and decouples them from the abundant I spins (^1H); both of these effects enhance the rate of spin diffusion among the dilute spins by several orders of magnitude.[19,21] For a spin-lock field applied along the x axis in the rotating frame and exceeding the strength of the dipolar interactions, the zero-order average Hamiltonian during the spin-diffusion process in a static sample is given by

$$\overline{H}^{(0)}_{\text{static}} = s\sum_{j<k} b_{jk}(r_{jk},\vartheta_{jk})[3S_{jx}S_{kx}-(\mathbf{S}_j\cdot\mathbf{S}_k)], \tag{1}$$

where s is a scaling factor that equals $-\frac{1}{2}$ for an on-resonance, continuous-wave (cw) spin lock[6] and b_{jk} is a geometric factor

$$b_{jk}(r_{jk},\vartheta_{jk}) = -\left(\frac{\mu_0}{4\pi}\right)\left(\frac{\gamma_s^2\hbar}{r_{jk}^3}\right)\frac{1}{2}(3\cos^2\vartheta_{jk}-1)$$
$$= -d_{jk}P_2(\cos\vartheta_{jk}), \tag{2}$$

where $P_2(\cos\vartheta_{jk})=\frac{1}{2}(3\cos^2\vartheta_{jk}-1)$. ϑ_{jk} denotes the angle between the internuclear vector, $\mathbf{r}_{jk}$, of the spins j and k and the external magnetic field, and d_{jk} is the dipolar coupling constant.

The truncated Hamiltonian of Eq. (1) is rendered time dependent by sample rotation about an axis inclined at an angle Θ from the direction of $\mathbf{B_0}$.[17,22] Under the condition $|sb_{jk}| \ll \omega_r \ll \omega_{1S}$, average Hamiltonian theory can again be applied to the Hamiltonian already truncated by the rf field, and the secular (zeroth-order) Hamiltonian for the spin-diffusion process in the rotating sample becomes

$$\overline{H}^{(0)}_{\text{rot}} = P_2(\cos\Theta)H_S, \tag{3}$$

with

$$H_S = s\sum_{j<k} b_{jk}(r_{jk},\beta_{jk})[3S_{jx}S_{kx}-(\mathbf{S}_j\cdot\mathbf{S}_k)].$$

 0021-9606/98/108(3)/826/4/$15.00

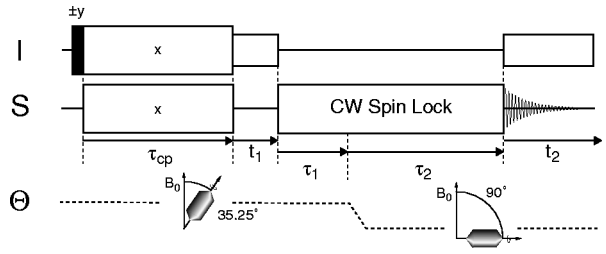

FIG. 1. Pulse sequence for refocusing rf-driven spin diffusion by sample reorientation. Hartmann–Hahn cross polarization (Refs. 24, 25) is used to enhance the polarization of the S spins. The S spins are frequency labeled during the evolution time, t_1. For the entire mixing period, spin diffusion among the S spins is driven by a cw spin lock (Refs. 19, 20). In the defocusing period, τ_1, the sample is spun at the angle $\Theta_1 = 35.25°$. During the refocusing time, τ_2, the rotation axis is rapidly reoriented to $\Theta_2 = 90°$, and the rf-driven spin diffusion is time reversed at $\tau_2 = \tau_1$. Proton decoupling is applied during both the evolution (t_1) and detection (t_2) periods.

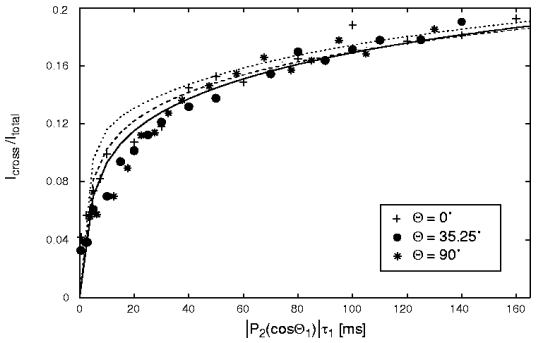

FIG. 2. Experimental build-up of the normalized rf-driven spin diffusion cross-peak intensity in ^{13}C natural-abundance adamantane as a function of $|P_2(\cos\Theta_1)|\times\tau_1$ for $\Theta_1 = 0°$, 35.25°, and 90°. Experimental parameters are given in the caption of Fig. 3. The curves were numerically calculated from a kinetic master equation for the polarization exchange process [Eq. (7)]. An fcc lattice of 1000 adamantane molecules was constructed with a nearest distance of 6.6 Å between molecular centers (Ref. 34). Due to the fast rotational dynamics of adamantane molecules at 300 K, the *intramolecular* dipolar interactions are averaged to zero, and the observed polarization transfer reflects only *intermolecular* dipolar interactions. The S-spin lattice sites (in the center of gravity of the rotating molecule) were occupied by using a random number generator and considering the probabilities of $^{13}CH_2$ and ^{13}CH occurrence at natural abundance (Ref. 35). It was assumed that no more than two ^{13}C atoms were present in a single molecule. The matrix elements, W_{jk}, of $\tilde{\mathbf{W}}$ were evaluated separately for each dipolar-coupled spin pair using Eq. (5) with $\Theta_1 = 0°$. The three curves represent three different model assumptions used for the evaluation of W_{jk}. The dotted curve was generated using the approximation that $\langle(1-3\cos^2\beta_{jk})^2\rangle_{\text{powder}} = 4/5$ for each spin pair (Ref. 14). The dashed curve was obtained by performing an explicit powder average over 1000 orientations using the method of Cheng *et al.* (Ref. 36). The solid curve was obtained by additionally taking into account the fast rotational diffusion of the adamantane molecules on their lattice sites which leads to a motionally averaged internuclear distance $\langle r_{jk}\rangle$ and angle $\langle\beta_{jk}\rangle$ (Ref. 35). All three curves represent an average over 100 different randomly occupied S-spin lattices. Qualitative agreement with the experimental data is obtained when a uniform and constant normalized zero-quantum intensity of $F_{jk}(0) = F(0) = (7\pm2)\times10^{-2}$ s is assumed. This leads to a linewidth of the normalized S spin zero-quantum spectrum of 10–14 Hz assuming a Lorentzian or Gaussian shape.

Here, $b_{jk}(r_{jk},\beta_{jk})$ has the same functional form as Eq. (2) except the relevant angle, β_{jk}, is the one between the internuclear vector and the rotor axis. In the case of magic-angle spinning, $P_2(\cos 54.74°)$ equals zero, and the spin diffusion is quenched without the application of recoupling sequences.[9,23]

The form of the scaling term $P_2(\cos\Theta)$ in Eq. (3) provides the possibility of switching the sign of the Hamiltonian that governs rf-driven spin diffusion by changing the orientation of the rotor axis relative to $\mathbf{B_0}$. The rf-pulse sequence shown in Fig. 1 takes advantage of this property and represents a polarization-echo experiment.[7,9] Cross polarization[24,25] is used to polarize the S spins during a preparation period τ_{cp} while the sample is spun about an axis oriented at the angle $\Theta_1 = 35.25°$ relative to $\mathbf{B_0}$. After a frequency-labeling period t_1, a cw spin lock is applied. For a time τ_1, rf-driven spin diffusion occurs under the Hamiltonian of Eq. (3) with $P_2(\cos 35.25°) = 0.5$. During the time τ_2, the sample is rapidly reoriented to $\Theta_2 = 90°$, and the spins evolve under a driving Hamiltonian with a scaling factor of $P_2(\cos 90°) = -0.5$. The signal is then acquired for a time t_2. It is easily seen that the propagator $e^{-iP_2(\cos\Theta_1)H_S\tau_1}e^{-iP_2(\cos\Theta_2)H_S\tau_2}$ is the unity operator if $\tau_1 = \tau_2$, and an echo occurs at that point in time, even for many-body interactions. Obviously, an echo can also be formed with other combinations of the angles Θ_1 and Θ_2. Although a polarization echo could be observed in a one-dimensional experiment with selective excitation, we use here a two-dimensional experiment[26] which allows one to distinguish the contributions of spin diffusion from those of $T_{1\rho}$ relaxation in a single experiment.

The build-up of the cross-peak intensity during the time τ_1 with $\tau_2 = 0$ (see Fig. 1) scales linearly with $|P_2(\cos\Theta_1)|$ because the observable polarization on a given spin packet A,

$$\langle F_X^A(\tau_1)\rangle = \frac{\mathrm{Tr}\{e^{-i\overline{H}_{\text{rot}}^{(0)}\tau_1}\sigma(\tau_1=0)e^{i\overline{H}_{\text{rot}}^{(0)}\tau_1}F_X^A\}}{\mathrm{Tr}\{(F_X^A)^2\}} = \sum_{n=0}^{\infty}\frac{(-i)^n(\tau_1 P_2(\cos\Theta_1))^n}{n!}M_n, \qquad (4)$$

is determined by the *product* of $P_2(\cos\Theta_1)$ and τ_1. The M_n denote the moments of the series expansion.[6,14,17] In Eq. (4) we have interpreted the rf-driven spin diffusion as a deterministic unitary quantum-mechanical process described by the Hamiltonian $\overline{H}_{\text{rot}}^{(0)}$. The scaling behavior can be verified experimentally by observing ^{13}C rf-driven spin diffusion in polycrystalline adamantane for different values of $P_2(\cos\Theta_1)$. The largest value for $|sb_{jk}|/2\pi$ is 11 Hz for the carbons in natural-abundance adamantane so the condition $|sb_{jk}| \ll \omega_r \ll \omega_{1S}$ can easily be satisfied. In our experiments, $\omega_r/2\pi = 5.3$ kHz and $\omega_{1S}/2\pi = 20$ kHz. Figure 2 shows the build up of the normalized cross-peak intensity from rf-driven spin diffusion in adamantane as a function of $|P_2(\cos\Theta_1)|\times\tau_1$ for three different angles Θ_1. To within experimental error, all three sets of data points lie on the same curve.

The same scaling behavior results when first-order, time-dependent perturbation theory[14,27,28] is used to describe the polarization-transfer process. The spin-diffusion transition probability, P_{jk}, between two spins S_j and S_k can be written as[14,27]

$$P_{jk}(\tau_1) = W_{jk}\tau_1 = \frac{\pi}{2}s^2(P_2(\cos\Theta_1))^2 b_{jk}^2 F_{jk}(0)\cdot\tau_1. \qquad (5)$$

Here, $F_{jk}(0)$ is the intensity of the normalized zero-quantum

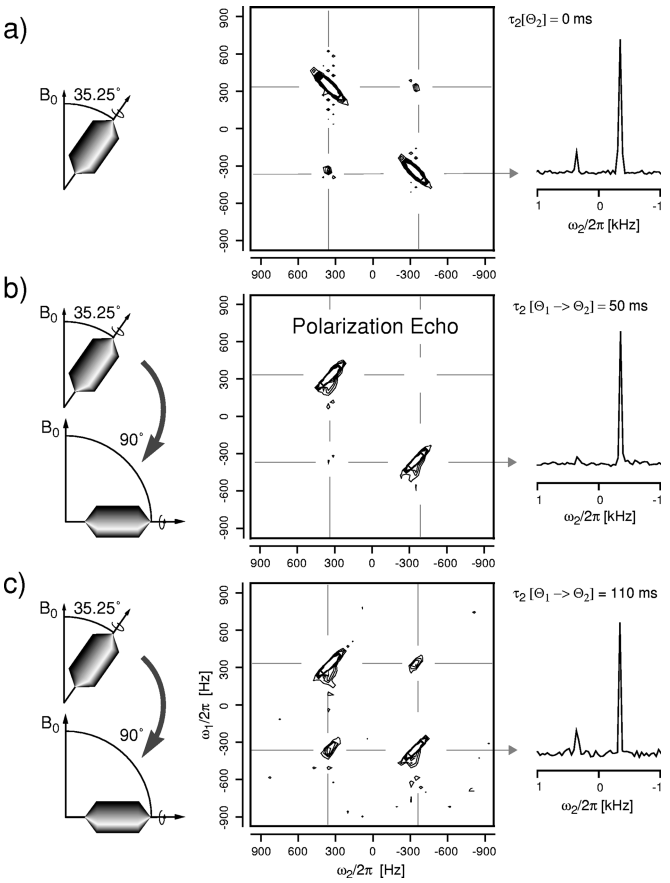

FIG. 3. Experimental two-dimensional ^{13}C rf-driven spin-diffusion spectra of adamantane. The spectra were recorded on a home-built spectrometer with a ^{13}C Larmor frequency of 75.7 MHz. Adamantane was purchased from Aldrich and used without further purification. A doubly tuned, home-built probe with a stationary coil and a moveable stator was used, and the angle of the rotor axis, Θ, was controlled by a stepper motor as described in Ref. 31. The amount of time necessary to reorient the sample was approximately 10 ms. The spinning speed was 5.3 kHz, and the rf field strengths were $\omega_{11}/2\pi=\omega_{1S}/2\pi=20$ kHz. The ^{13}C carrier frequency was positioned exactly between the two ^{13}C resonances in adamantane for the most efficient chemical-shift scaling during the cw-driven spin-diffusion period (Refs. 19–21). For the two-dimensional spectra, 90 complex t_1 points consisting of 16 scans each were collected according to the method of States *et al.* (Ref. 37). The delay between experiments was 3.5 s. (a) Rf-driven spin-diffusion spectrum obtained at $\Theta_1=35.25°$ (no axis reorientation) with a mixing time of $\tau_1=30$ ms. Cross peaks due to spin diffusion are visible. (b) Echo experiment obtained using the pulse sequence of Fig. 1 with $\tau_1=30$ ms and $\tau_2=50$ ms. The spin diffusion has been refocused, and the cross-peak intensity is nearly zero. Note that the orientation of the diagonal peaks has changed due to the sign change of $P_2(\cos\Theta)$ (which affects residual chemical shift, dipolar, and bulk susceptibility interactions during the evolution and detection periods). (c) Experiment obtained using the pulse sequence of Fig. 1 with $\tau_1=30$ ms and $\tau_2=110$ ms. The longer evolution at the second angle led to a recovery of the cross-peak intensities. In all three spectra, the contours are at 3%, 5%, 7%, 9%, 11%, 13%, and 15% of the maximum signal intensity.

spectrum of the spins S_j and S_k at frequency zero.[14,21,29] In the ideal case of rf-driven spin diffusion, the abundant I spins are completely decoupled from the S spins and, therefore, $F_{jk}(0)$ scales with $|sP_2(\cos\Theta_1)b_{jk}|^{-1}$. This leads to

$$P_{jk}(\tau_1)\propto|sb_{jk}|\cdot\tau_1|P_2(\cos\Theta_1)|. \tag{6}$$

Equations (5) and (6) predict that the rf-driven spin-diffusion rate constant, W_{jk}, scales with $1/r_{jk}^3$ in contrast to the proton-driven case where W_{jk} is proportional to $1/r_{jk}^6$.[21,29]

It is interesting to compare the experimental polarization-transfer dynamics with statistical predictions. The three curves shown in Fig. 2 result from a phenomenological model of the spin-diffusion process in natural-abundance ^{13}C admantane assuming a master equation for the polarization ($p_i=\langle S_{ix}\rangle$) exchange

$$\frac{d}{dt}\,\mathbf{p}=\tilde{\mathbf{W}}\cdot\mathbf{p}. \tag{7}$$

$\tilde{\mathbf{W}}$ represents the polarization-exchange matrix where W_{jk} is evaluated according to Eq. (5) with $\Theta_1=0°$ and the diagonal elements are defined as $W_{jj}=-\Sigma_{k\neq j}W_{kj}$ to conserve the sum polarization. The time dependence of the polarization transfer is nonexponential due to the statistical distribution of the ^{13}C spins on the lattice sites. For $\tau_1\leqslant 30$ ms, the ^{13}CH and $^{13}CH_2$ pairs on neighboring molecules predominantly contribute to the cross-peak intensities. For longer times, more remote spin packets (within the next nearest neighbor shell for the plotted time range) start to contribute as well, leading to a flattening of the build-up curve. Due to the isotropic dilution and the crystal structure of adamantane, the spin-diffusion dynamics appear to follow the predictions made for coupled clusters of spins.[30] Details of the model are given in the caption of Fig. 2.

To implement the echo pulse sequence of Fig. 1, we used a probe design in which a stationary coil surrounds a movable stator,[31] allowing continuous application of the rf spin lock during the mechanical hop. It was not possible to avoid irradiating the S spins during the hop by using $\pi/2$ storage pulses[32] since the full dipolar order could not be retained.[33] Figure 3 shows a set of two-dimensional spectra of adamantane obtained with $\tau_1=30$ ms and different values of τ_2. In Fig. 3(a), $\tau_2=0$ ms and the sample was spun at $\Theta_1=35.25°$, so rf-driven spin diffusion proceeded according to the Hamiltonian of Eq. (3) with $P_2(\cos\Theta_1)=0.5$. The spin-diffusion cross peaks are clearly visible. Figure 3(b) shows the spectrum corresponding to the polarization echo. In this experiment, the S-spin system evolved under a Hamiltonian with $P_2(\cos\Theta_1)=0.5$ for $\tau_1=30$ ms. The sample was then reoriented, and the evolution continued with $P_2(\cos\Theta_2)=-0.5$ for $\tau_2=50$ ms. The opposite signs of the scaling factor during τ_1 and τ_2 caused the evolution of the polarization transfer to refocus, and the cross-peak intensity approached zero. Since a finite time was required for the sample reorientation, the polarization echo was delayed and occurred at $\tau_2\approx 1.3\tau_1$. Figure 3(c) shows the case in which $\tau_2\gg\tau_1$, so the cross-peak intensity has recovered, reaching a value exceeding that shown in Fig. 3(a).

The complete time evolution of the echo is depicted in Fig. 4. The normalized cross-peak intensities are plotted as a function of total mixing time for $\tau_1=30$ ms [Fig. 4(a)] and $\tau_1=70$ ms [Fig. 4(b)]. For the experiments with the shorter τ_1 time, the refocusing of the spin diffusion is nearly complete, but at longer times the echo is weaker in amplitude. The reason for this is unclear. One possibility is that the strength of the ^{13}C rf field used in these experiments ($\omega_{1S}/2\pi=20$ kHz) may not be sufficient to fully decouple

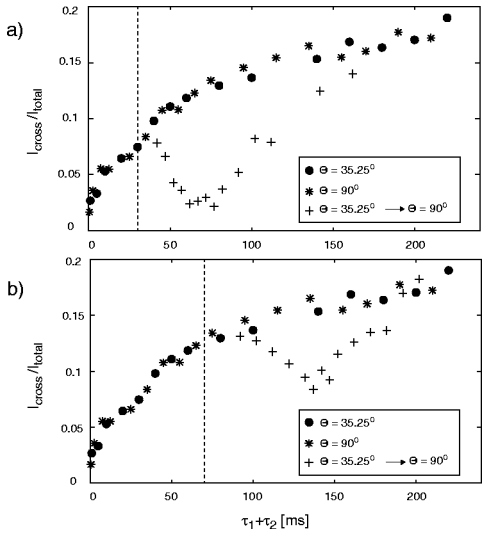

FIG. 4. Time evolution of the normalized cross-peak intensity in adamantane. The experimental parameters are the same as those listed in the caption of Fig. 3. The circles and asterisks show the cross-peak build-up as a function of mixing time for rf-driven spin diffusion at angles of $\Theta_1 = 35.25°$ and 90°, respectively. The crosses show the cross-peak intensities as a function of time for the echo experiment of Fig. 1 with (a) $\tau_1 = 30$ ms and (b) $\tau_1 = 70$ ms. The time at which the hop is initiated is indicated by a vertical line in each graph.

the abundant proton spins. Consequently, the S-spin polarization echo amplitude will be damped. The echo in Fig. 4(a) is broadened due to the finite time required for sample reorientation. The evolution during the reorientation is difficult to quantify since it is not known precisely how much time the sample spends at each angle. Furthermore, the scaling factor, $P_2(\cos\Theta)$, varies nonlinearly with Θ, and the sign change occurs at an angle ($\Theta = 54.74°$) that is closer to 35.25° than to 90°. For these reasons, the echo position will be sensitive to instabilities in the mechanical reorientation process, leading to a broadening of the echo maximum for $\tau_1 \geqslant \tau_{\mathrm{hop}}$.

In summary, a type of polarization echo, which is based on the manipulation of the spatial part of the dipolar Hamiltonian, is introduced in this communication. We have experimentally demonstrated that the spin-diffusion process can be refocused by a mechanical sample reorientation. Rf-driven ^{13}C polarization echoes were observed for mixing times on the order of 100 ms, more than 2 orders of magnitude longer than the time scale for previously observed proton dipolar echoes.[7,9] Although rf-driven spin diffusion in adamantane can be qualitatively described by a master equation for polarization exchange, such an approach obviously fails to describe the formation of the echoes.

This work was supported by the Director, Office of Energy Research, Office of Basic Energy Sciences, Materials Sciences Division, U. S. Department of Energy, under Contract No. DE-AC03-76SF00098. Support from SON and the SON HF-NMR Facility, University of Nijmegen is gratefully acknowledged. M.T. acknowledges support from the Swiss National Foundation of Science. We are grateful to Professor Richard R. Ernst and Gabriele Aebli for discussions and comments.

[a]Present address: Max-Planck-Institut für Polymerforschung, Postfach 3148, D-55021 Mainz, Germany.

[1] E. L. Hahn, Phys. Rev. **80**, 580 (1950); S. L. McCall and E. L. Hahn, *ibid.* **183**, 457 (1969); M. P. Augustine and E. L. Hahn, J. Chem. Phys. **107**, 3324 (1997).
[2] H. Schneider and H. Schmiedel, Phys. Lett. **30A**, 298 (1969).
[3] W.-K. Rhim, A. Pines, and J. S. Waugh, Phys. Rev. Lett. **25**, 218 (1970).
[4] A. Llor, Z. Olejniczak, J. Sachleben, and A. Pines, Phys. Rev. Lett. **67**, 1989 (1991).
[5] N. Bloembergen, Physica (Utrecht) **15**, 386 (1949).
[6] C. P. Slichter, *Principles of Magnetic Resonance* (Springer-Verlag, Berlin, 1990).
[7] S. Zhang, B. H. Meier, and R. R. Ernst, Phys. Rev. Lett. **69**, 2149 (1992).
[8] T. Karlsson, M. Helmle, N. D. Kurur, and M. H. Levitt, Chem. Phys. Lett. **247**, 534 (1995).
[9] M. Tomaselli, S. Hediger, D. Suter, and R. R. Ernst, J. Chem. Phys. **105**, 10672 (1996).
[10] E. R. Andrew, A. Bradbury, and R. G. Eades, Nature (London) **182**, 1659 (1958).
[11] I. J. Lowe, Phys. Rev. Lett. **2**, 285 (1959).
[12] D. P. Raleigh, M. H. Levitt, and R. G. Griffin, Chem. Phys. Lett. **146**, 71 (1988).
[13] M. G. Colombo, B. H. Meier, and R. R. Ernst, Chem. Phys. Lett. **146**, 189 (1988).
[14] A. Abragam, *Principles of Nuclear Magnetism* (Clarendon Press, Oxford, 1961).
[15] M. Goldman, *Spin Temperature and Nuclear Magnetic Resonance in Solids* (Oxford University Press, London, 1970).
[16] M. Ernst and B. H. Meier, in *Solid State NMR of Polymers*, edited by I. Ando and T. Askura (Elsevier Science, New York, in press).
[17] M. Mehring, *Principles of High-Resolution NMR in Solids* (Springer-Verlag, Berlin, 1976).
[18] H. Schmiedel, B. Hillner, and S. Grande, Phys. Lett. **78A**, 458 (1980).
[19] P. Robyr, B. H. Meier, and R. R. Ernst, Chem. Phys. Lett. **162**, 417 (1989).
[20] P. Robyr, M. Tomaselli, J. Straka, C. Grob-Pisano, U. W. Suter, B. H. Meier, and R. R. Ernst, Mol. Phys. **84**, 995 (1995).
[21] B. H. Meier, Adv. Magn. Opt. Reson. **18**, 1 (1994).
[22] E. R. Andrew, A. Bradbury, and R. G. Eades, Nature (London) **183**, 1802 (1959).
[23] M. Baldus, M. Tomaselli, B. H. Meier, and R. R. Ernst, Chem. Phys. Lett. **230**, 329 (1994).
[24] S. R. Hartmann and E. L. Hahn, Phys. Rev. **128**, 2042 (1962).
[25] A. Pines, M. G. Gibby, and J. S. Waugh, J. Chem. Phys. **59**, 569 (1973).
[26] R. R. Ernst, G. Bodenhausen, and A. Wokaun, *Principles of Nuclear Magnetic Resonance in One and Two Dimensions* (Clarendon Press, Oxford, 1987).
[27] J. J. Sakurai, *Modern Quantum Mechanics* (Addison-Wesley, Redwood City, 1985).
[28] K. Schmidt-Rohr and H. W. Spiess, *Multidimensional Solid-State NMR and Polymers* (Academic, San Diego, 1994).
[29] D. Suter and R. R. Ernst, Phys. Rev. B **32**, 5608 (1985).
[30] L. Emsley and A. Pines, in *Proceedings of the International School of Physics (Enrico Fermi)* (Sociètà Italiana di Fisica: Varenna on Lake Como, 1992).
[31] K. T. Mueller, G. C. Chingas, and A. Pines, Rev. Sci. Instrum. **62**, 1445 (1991).
[32] K. T. Mueller, B. Q. Sun, G. C. Chingas, J. W. Zwanziger, T. Terao, and A. Pines, J. Magn. Reson. **86**, 470 (1990).
[33] J. H. Baltisberger, S. L. Gann, P. J. Grandinetti, and A. Pines, Mol. Phys. **81**, 1109 (1994).
[34] W. Nowacki, Helv. Chim Acta **28**, 1233 (1945).
[35] C. E. Bronniman, N. M. Szeverenyi, and G. E. Maciel, J. Chem. Phys. **79**, 3694 (1983).
[36] V. B. Cheng, H. H. Suzukawa, Jr., and M. Wolfsberg, J. Chem. Phys. **59**, 3992 (1973).
[37] D. J. States, R. A. Haberkorn, and D. J. Ruben, J. Magn. Reson. **48**, 286 (1982).